Carbohydrate Polymers 88 (2012) 904–911

Contents lists available at SciVerse ScienceDirect

Carbohydrate Polymers

journal homepage: www.elsevier.com/locate/carbpol

Calcium phosphates synthesized by reverse emulsion method for the preparation of chitosan composite membranes

Hung-Yin Tai [a], Earl Fu [b], Trong-Ming Don [a,*]

[a] Department of Chemical and Materials Engineering, Tamkang University, Tamsui District, New Taipei City 25137, Taiwan
[b] Department of Dentistry, National Defense Medical Center and Tri-service General Hospital, Neihu District, Taipei City 114, Taiwan

ARTICLE INFO

Article history:
Received 14 November 2011
Received in revised form 12 January 2012
Accepted 13 January 2012
Available online 23 January 2012

Keywords:
Chitosan
Calcium phosphate
Composite membranes

ABSTRACT

Calcium deficient hydroxyapatite (CDHA) having an average particle size of 45 nm was synthesized by reverse emulsion method. It was converted to the respective biphasic calcium phosphate (BCP, 226 nm) and β-tricalcium phosphate (TCP, 450 nm) by calcination at 800 °C and 1000 °C, and the BCP consisted of 92% TCP and 8% CDHA. Subsequently, chitosan was mixed with calcium phosphates to prepare CDHA/chitosan, BCP/chitosan, and TCP/chitosan membranes. The initial moduli of the BCP/chitosan and TCP/chitosan membranes were about 1.9 times that of the pure chitosan membrane; and the elongations at break were almost 6 times. The CDHA/chitosan and BCP/chitosan could induce mineralization of apatite on the membranes by increasing 20.6 and 16.3 wt.%, respectively, after 24 days in the simulated body fluid. Moreover, the BCP/chitosan exhibited superior osteoblast cell attachment and proliferation than the other membranes. It has the potential to be used as the barrier membrane for guided bone regeneration.

1. Introduction

Periodontitis is caused by some inflammatory diseases that could result in a progressive retrograde of the alveolar bone. In order to overcome this problem, periodontal tissue engineering using biomaterial-based therapy to restore bone tissue has been developed (Behring, Junker, Walboomers, Chessnut, & Jansen, 2008; Imbronito, Todescan, Carvalho, & Arana-Chavez, 2002; LeGeros, 2008). The approach of periodontal tissue engineering is considered promising to restore bone defect through the use of engineered materials with the aim that they will prohibit the invasion of fibrous connective tissue and help repair the function during bone regeneration (Behring et al., 2008). In this regard, these engineered materials are named barrier membranes in periodontal tissue engineering. Successful barrier membranes thus require several specific properties including selective permeability to prohibit the invasion of fibrous connective tissue, excellent bone affinity to guide bone regeneration, good mechanical strength to maintain a secluded space for bone regeneration and suitable degradability to prevent secondary surgical (Imbronito et al., 2002).

Bioresorbable polymers therefore are more advantageous than nondegradable polymers for preventing a secondary surgical (Imbronito et al., 2002). Among various bioresorbable polymers, chitosan is recognized as a potential barrier membrane for periodontitis because it also has biocompatibility and bone affinity (Burg, Porter, & Kellam, 2000; Etienne et al., 2005). Nowadays, chitosan gels and films have been applied in various fields including wound-dressing, drug controlled release, and tissue engineering (Hamilton et al., 2007; Rinaudo, 2006). Fakhry, Schneider, Zaharias, and Senel (2004) found that chitosan had better cell attachment and spreading of osteoblasts over fibroblasts. Hamilton et al. (2007) used various chitosan materials to prepare membranes. They found that although the chitosan membranes used in the study had different degrees of deacetylation and different molecular weights, they all could support high levels of bone cell proliferation. The results thus suggest that chitosan-based materials have potential to be used in periodontal application.

While chitosan is a biocompatible substrate for tissue propagation and is potentially an effective membrane in the repair of bone defects, there is still a need for further improving the bone affinity and mechanical properties of chitosan membranes. Considering that bone is a nanocomposite consisting of nanoscale minerals of biological apatite and a matrix of collagen, proteoglycans, and glycoprotein (Grynpas & Omelon, 2007), various calcium phosphate ceramics have been proposed and extensively studied as candidates for inducing bone regeneration. Especially, hydroxyapatite (HA), $Ca_{10}(PO_4)_6(OH)_2$, and tricalcium phosphate (TCP), $Ca_3(PO_4)_2$, are the two most important calcium phosphate ceramics for bone engineering (LeGeros, 2008). HA chemically resembles the inorganic component of human bone and is considered as an osteoconductive

* Corresponding author. Tel.: +886 2 26293856; fax: +886 2 26209887.
E-mail address: tmdon@mail.tku.edu.tw (T.-M. Don).

0144-8617/$ – see front matter © 2012 Elsevier Ltd. All rights reserved.
doi:10.1016/j.carbpol.2012.01.042

and bioactive ceramic (Chow & Eanes, 2001). On the other hand, TCP is considered as a bioresorbable ceramic which can be gradually replaced by new functional bone due to its phenomenal bioresorbability in biological environments (Dasgupta & Bose, 2009). Additionally, some attempts have been made to develop biphasic calcium phosphate (BCP) from a mixture of HA and TCP (Arinzeh, Tran, Mcalary, & Daculsi, 2005; Vallet-Regí, 2001). Since the BCP contained the TCP component, it could also gradually dissolve in the body, releasing Ca^{2+} and PO_4^{3-} to the local environment and acting as a stem to form new bone (Vallet-Regí, 2001).

Several studies have been reported on the preparation and properties of chitosan/calcium phosphate composite membranes (Aylin & Russell, 2007; Chesnutt et al., 2009; Kuo et al., 2009). Chesnutt et al. (2009) used co-precipitation method to prepare chitosan/HA scaffold. The cell proliferation was significantly increased when osteoblast was cultured on the chitosan/HA composite scaffold compared to that on the pure chitosan. Kuo et al. (2009) found that the chitosan membranes incorporated with TCP could give better bone healing than the pure chitosan membrane on the bone defect after 4 weeks of recovering. Aylin and Russell (2007) suggested that the use of biphasic calcium phosphate (BCP) composed of HA and TCP as a means for enhancing the osteoconductivity of the chitosan scaffold for bone tissue engineering application. However, there is still no report on the direct comparison of the chitosan composite membranes incorporated with different calcium phosphates of HA, TCP, and BCP. Thus, our objective here is to present a systematic study in describing the synthesis and structure characterization of different calcium phosphates obtained by reverse emulsion method (water in oil, W/O), as well as the mechanical properties and biological responses of the chitosan composite membranes with the as-prepared calcium phosphates, in the effort to develop nanocomposite barrier membranes for periodontal tissue engineering.

2. Experimental

2.1. Synthesis of calcium phosphate particles

Reverse emulsion method was used to prepare calcium phosphate nanoparticles. First, the calcium solution and the phosphate solution were prepared separately by dissolving the required amounts of the respective calcium nitrate ($Ca(NO_3)_2{\cdot}4H_2O$, Sigma–Aldrich, USA) and diammonium hydrogen phosphate ($(NH_4)_2HPO_4$, Sigma–Aldrich, USA) in distilled water. The molar ratio of Ca to P was controlled at 1.5. In the mean time, the surfactant, Span 80 (Fluka, USA), was added into the cyclohexane (Sigma–Aldrich, USA) at a concentration of 4% to prepare the oil phase. The two aqueous solutions were then dropped into the oil phase separately. The volume ratio of each aqueous phase to the oil phase was fixed at 1/5. After sonication for 5 min to produce water in oil emulsion, the two emulsions were mixed together and sonicated again. The pH value was maintained at 10 in the whole process by dripping ammonium hydroxide solution. The final emulsion was aged at room temperature for 24 h. It was then washed by MeOH to remove the residual Span 80 and dried at 95 °C. The as-dried particles were further heated to 800 °C or 1000 °C at a heating rate of 5 °C/min and maintained at that temperature for 30 min in a muffle furnace (Thermo Scientific, USA). They were then cooled down to room temperature in the furnace.

2.2. Preparation of chitosan/calcium phosphate composite membranes

Chitosan was purchased from Tokyo Chemical Incorporation (Tokyo, Japan). After purification, chitosan had a molecular weight of 350,000 g/mol and deacetylation of 86% (Don, Chou, Cheng, & Tai, 2011). The chitosan solution with 2 wt.% was first prepared in a 0.5% (w/v) acetic acid aqueous solution, and it was then added with the prepared calcium phosphate particles. The mixture was stirred at 50 °C for 9 h to obtain a dispersion solution. Approximately 8 g of this dispersion solution was poured into a Teflon dish with a diameter of 8 cm and dried in a ventilation oven at 40 °C for 24 h. The obtained calcium phosphate/chitosan membrane was neutralized with a basic solution, $NaOH_{(aq)}$, and then washed with a great amount of distilled water until pH 7.0. It was then oven-dried at 40 °C again. All membranes with a diameter of 7.5 ± 0.3 cm and a thickness of 30 ± 5 μm were thus obtained by direct drying in the oven. The weight ratio of the calcium phosphate to the chitosan matrix was fixed at 3/10. For comparison, pure chitosan membrane without calcium phosphate was also prepared with the same procedure.

2.3. Characterizations of calcium phosphates and composite membranes

The micelle size in the emulsion and particle size of the prepared calcium phosphates were determined by dynamic light scattering (DLS) using Zetasizer (Nano ZS, Malvern, UK). X-ray diffractometer (XRD, D8-Advance, Bruker, Germany) employing the Cu-Kα radiation was used to examine the structures of the synthesized calcium phosphates as well as the chitosan composite membranes. The diffractometer was operated at 45 kV and 40 mA over the 2θ range of 5–60°. The particle texture of calcium phosphates was examined using transmission electron microscope (TEM, EM-2100F, JEOL, Japan). The morphology of composite membranes was examined using a scanning electron microscope (FESEM, Leo 1530, Oberkochen, Germany). Samples were coated by a very thin layer of platinum before taking their SEM images. The average size of the calcium phosphate particles on the composite membranes was determined from thirty different particles shown on the SEM pictures using Image-Pro Plus software (Media Cybernetics, USA). Energy dispersive spectrometer (EDS) was used to characterize chemical elements of the synthesized calcium phosphate ceramics and especially their Ca/P ratios. Furthermore, tensile mechanical properties of the composite membranes were measured at room temperature using an Autograph AGS-J series universal tester (Shimadzu, Japan). The membranes with thickness about 30 μm were cut into the standard tensile specimens. The cross-head speed was set at 2 mm/min. The stress and strain were measured continuously and tensile mechanical properties including initial modulus (E), ultimate tensile strength (UTS), and elongation at break (ε_b, %) were calculated from the stress–strain curves. More than five specimens were tested under each condition, and the results were averaged.

2.4. In vitro assays in simulated body fluid

In order to assess the *in vitro* bioactive behavior of each composite membrane, the membrane with a diameter of 1.5 cm was immersed in a simulated body fluid (SBF) at 37 °C. The SBF is the most favored model solution for the evaluation of bioactivity of material by assessing the ability to induce apatite formation. The SBF is an acellular solution containing the following chemicals (Müler & Müler, 2006): NaCl (136.8 mM), $NaHCO_3$ (4.2 mM), KCl (3.0–5.0 mM), K_2HPO_4 (1.0 mM), $MgCl_2{\cdot}6H_2O$ (1.5 mM), $CaCl_2$ (2.5 mM) and Na_2SO_4 (0.5 mM). These chemicals were mixed together and buffered at pH 7.3 with hydrochloric acid/tris(hydroxymethyl)aminomethane (Sigma–Aldrich, USA). The SBF solution was filtered in a 0.22 μm Millipore system to avoid biological contamination. Each sample was incubated in 50 mL of the SBF solution in an incubator-shaker with a circular motion at 70 rpm. The changes of Ca^{2+} concentration in the SBF solution

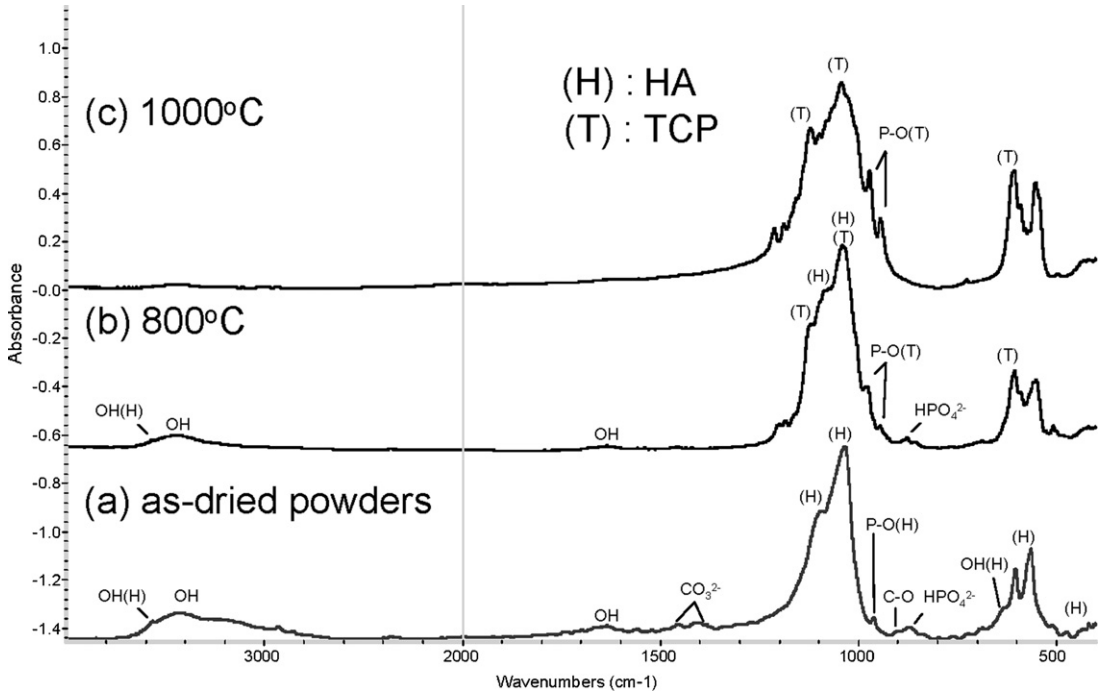

Fig. 1. Fourier transforms infrared (FTIR) spectra of the as-dried particles from the reverse emulsion method (a), and the particles being further calcined at 800 °C (b) and 1000 °C (c).

after immersion of the composite membrane at 1, 3, 7, 14, and 24 days were measured by an atomic absorption spectrophotometer (Shimadzu, Japan). In addition, after 24 days of immersion, the membranes were removed from the SBF, slightly rinsed with water and then acetone, and finally dried in the ventilation hood at room temperature. These membranes were then characterized by SEM and XRD.

2.5. In vitro test of osteoblast cell attachment and proliferation

Primary osteoblast (OB) cells were obtained from the parietal bones of calvaria of SD rats in this study. They were suspended in the LG-DMEM (low glucose, Gibco/Invitrogen, California, USA) supplemented with 10% fetal bovine serum (Gibco/Invitrogen, California, USA) and 1% penicillin/streptomycin (Gibco/Invitrogen, California, USA) as the medium, and cultured in a humidified atmosphere of 95% air and 5% CO_2 at 37 °C. Culture medium was renewed every 2 days. The cells forming a monolayer were detached from the plate by adding 0.5% trypsin at 37 °C for 1 min and resuspended in the culture medium. Cell number was counted by the microscopy using a Neubauer hemocytometer. The tested membrane was placed on a tissue-culture-treated polystyrene plate and fixed with a silicone ring. The OB cells (5×10^4 cells in 1 mL) were then pipetted onto the surface of the membrane. Both cell attachment and cell proliferation were evaluated. After culturing at a specific time interval, the membrane was washed by D-PBS to remove the unattached OB cells. The number of the residual cells on the membrane was determined by MTS assay (Cell Titer 96 Aqueous One Solution, Promega, USA). Each membrane was dispensed with 100 μL culture medium and 20 μL MTS with a micropipette and then incubated at 37 °C for 4 h. The absorbance at 490 nm was measured using an enzyme-linked immunosorbent assay with a Multiskan Spectrum Microplate Spectrophotometer (Thermo science, UK), and it was then converted directly to the cell number using a standard curve. Data were collected and averaged from five specimens for each condition. The level of cell attachment was evaluated after culturing for 1, 2, 4, 5, and 6 h; whereas the level of cell proliferation was obtained after culturing for 1, 2, 3 and 4 days.

3. Results and discussion

3.1. Structure of calcium phosphate particles

Compared with other chemical routes, the emulsion method typically exhibits better control over nanoscale morphology. Therefore, calcium phosphate nanoparticles were produced by using reverse emulsion method (water in oil, W/O). When the calcium nitrate and ammonium phosphate aqueous solutions in the cyclohexane oil phase containing Span 80 were sonicated together, the produced W/O emulsion had numerous stable aqueous micelles with an average size of 220 nm. This is smaller than the size reported by Jarudilokkul, Tanthapanichakoon, and Boonamnuayvittaya (2007) who tried to produce HA nanoparticles by W/O/W emulsion system consisting of Span 20 and Tween 80. They found the emulsion droplet size distributions were in the range of 1–100 μm. Inside the micelles, nucleation of calcium phosphate ceramics occurred first due to the reaction of calcium nitrate and ammonium phosphate (Ca/P = 1.5) at pH 10. Fig. 1(a) presents the FTIR spectrum of the produced calcium phosphate particles. The characteristic PO_4^{3-} and OH^- absorption peaks of HA are observed. Yet, a weak absorption peak at 878 cm^{-1} is recognized as the P—O—H vibration in the HPO_4^{2-} group, which only exists in the non-stoichiometric apatite (Lin, Liao, Chen, Sun, & Lin, 2001). The hydroxyl group absorption bands are revealed to some degree at 3570 and 640 cm^{-1}. The absorption peaks at 890 and 1403–1456 cm^{-1} indicate the presence of carbonate group (CO_3^{2-}) which is commonly found in the synthesized apatite and natural bones. The results thus indicate that the as-synthesized particles have a structure of non-stoichiometric calcium deficient HA (CDHA). When the produced CDHA particles were further calcined at 800 °C, they underwent structure transformation to some extent. Fig. 1(b) reveals several new peaks at 1120, 1042, 971, 945

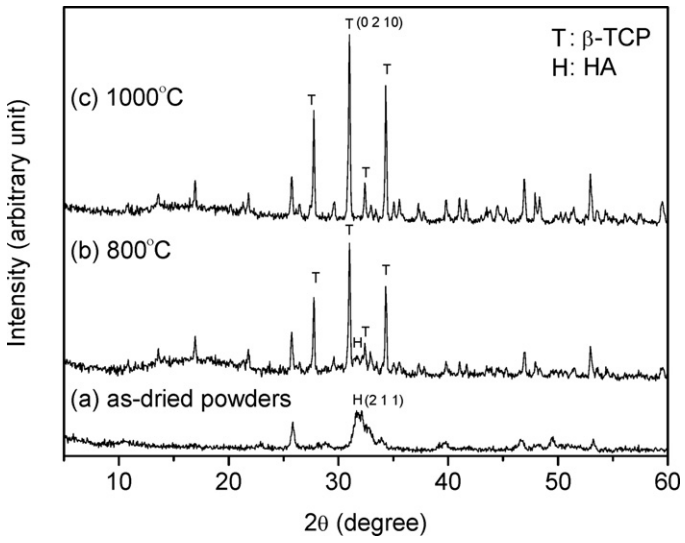

Fig. 2. XRD patterns of the as-dried particles from the reverse emulsion method (a), and the particles being further calcined at 800 °C (b) and 1000 °C (c).

and 606 cm^{-1} in the spectrum which are characteristic absorption peaks of TCP. However, the OH^- and HPO_4^{2-} peaks at 3570 and 878 cm^{-1}, with decreasing intensity, imply that the produced calcium phosphate is composed of CDHA and TCP, i.e. biphasic calcium phosphate (BCP). A complete transformation of CDHA to TCP was achieved when the CDHA was calcined at a higher temperature of 1000 °C. Fig. 1(c) clearly shows the distinct PO_4^{3-} peaks of the TCP at 971 and 944 cm^{-1} as well as the disappearance of the HPO_4^{2-} peaks of the CDHA.

The composition of the BCP could be estimated by its Ca/P ratio by knowing the Ca/P ratios of the individual CDHA and TCP. The EDS result shows that the produced CDHA has the Ca/P ratio of 1.347 ± 0.038, suggesting a chemical formula of $Ca_{8.08}(HPO_4)_{1.92}(PO_4)_{4.08}(OH)_{0.08}$ (Hench, 1998). On the other hand, the produced calcium phosphate by calcination at 1000 °C has the Ca/P ratio of 1.502 ± 0.043. Since the pure TCP has a theoretical Ca/P ratio of 1.50, the EDS result thus confirms that the produced calcium phosphate at 1000 °C is TCP. As the Ca/P ratios of the individual CDHA and TCP were known, the composition of the BCP was then calculated from its Ca/P ratio of 1.469 ± 0.048. The result shows that the BCP contains 92.2% of TCP and 7.8% of CDHA.

The structures of the synthesized calcium phosphates were further confirmed by XRD patterns. The as-dried calcium phosphate particles obtained from the reverse emulsion method has an apatite structure (Fig. 2(a), JCPDS file number 9-432). This agrees to the report from Pattanayak, Dash, Prasad, Rao, and Mohan (2007) that the synthesized ceramics would be apatite when the initial Ca/P ratio is in the range of 1.50–1.67. Fig. 2(b) shows the XRD pattern of the produced calcium phosphate at 800 °C. It can be seen that the apatite peak diminishes and the TCP peak (JCPDS file number 9-169) appears in strong intensity at diffraction angle $2\theta = 31.0°$. This demonstrates the existence of a biphasic calcium phosphate consisting of CDHA and TCP. Kwon, Jun, Hong, and Kim (2003) also found the similar behavior that the CDHA can be resolved into the stable TCP upon calcination at 800 °C. When the calcination temperature was increased to 1000 °C, single TCP phase was obtained (Fig. 2(c)). The XRD results thus agree with the FTIR and EDS analyses. It was proposed that the composition of the produced BCP could be estimated from the relative intensity ratio of the TCP peak (RIR_{TCP}) in the XRD pattern (Petrov, Dyulgerova, Petrov, & Popova, 2001). By using the following equation:

$$\mathrm{RIR_{TCP}} = \frac{I_{TCP}}{I_{CDHA} + I_{TCP}} \quad (1)$$

where I_{CDHA} and I_{TCP} represent the intensities of the CDHA peak (2 1 1) at 31.75° and the TCP peak (0 2 10) at 31.0°, the RIR_{TCP} value is obtained as 0.92, suggesting that the produced BCP is composed of 92% TCP and 8% CDHA, in agreement with the result obtained from the EDS analysis.

The morphology and the particle size of the produced calcium phosphate ceramics are shown in Fig. 3. It is clear that they have quit distinctive characteristics in shape, size, and size distribution. The produced CDHA has a needle-like structure and appears to have a slight aggregation. The average particle size is about 45 nm. However, the particles coarsen significantly when calcined at high temperatures. The CDHA transforms to the respective BCP with a rod-like structure and TCP with a spherical structure at 800 °C and 1000 °C. The average particle size is about 226 nm at 800 °C and increases up to 450 nm at 1000 °C. Simultaneously, the size distribution becomes broaden with higher calcination temperature as shown in Fig. 3(b). The same trend was also observed in the preparation of calcium phosphate nanopowder using reverse emulsion system consisting of poly(oxyethylene)$_5$ nonylphenol ether and poly(oxyethylene)$_{12}$ nonylphenol ether as the non-ionic surfactants (Dasgupta & Bose, 2009).

3.2. Characterization and in vitro bioactivity of chitosan composite membranes

In this study, organic/inorganic composite membranes were produced from the biodegradable chitosan with the prepared three different calcium phosphate particles (CDHA, BCP and TCP). Chitosan was used as the matrix to provide a barrier layer for tissue reconstruction. Calcium phosphate is composed of Ca^{2+} and PO_4^{3-}, and therefore it plays a role in guiding bone tissue regeneration (Hench, 1998). Fig. 4(a) shows the morphology of the chitosan membrane and the prepared calcium phosphate/chitosan composite membranes, all illustrating a smooth and dense structure. In addition, the CDHA, BCP, and TCP particles can be clearly observed in the respective composite membranes that they distribute uniformly in the chitosan matrix and the interface between the organic and inorganic phase is indistinguishable. This indicates that these calcium phosphate particles have a high affinity to the chitosan matrix. Moreover, the particle sizes of CDHA, BCP, and TCP in the composite membranes are found to be 37.6 ± 11.1 nm, 279.5 ± 36.0 nm, and 499.4 ± 33.0 nm, respectively, close to the values of original particles before mixing with the chitosan. It thus implies that the preparation of composite membranes would not affect the particle size.

Bioactivity is the required property of the bone-tissue-engineering material to be used as an implant in body application. In this study, *in vitro* bioactivity of the composite membranes was evaluated from the morphology changes of membranes after being immersed in the SBF for 24 days. Compared to Fig. 4(a), the SEM pictures in Fig. 4(b) reveal that some new inorganic particles deposited uniformly on the surface of the composite membranes after 24 days of immersion. Besides, more inorganic particles are found on the surface of the CDHA/chitosan and BCP/chitosan compared with the TCP/chitosan membrane. The increasing weight percentage due to the deposited inorganic particles on the membranes is on the order of CDHA/chitosan ($20.6 \pm 2.9\%$) > BCP/chitosan ($16.3 \pm 2.2\%$) > TCP/chitosan ($9.9 \pm 3.3\%$) > chitosan ($3.6 \pm 2.1\%$).

The crystalline structures of the composite membranes before and after immersion in the SBF were examined by XRD. For the pure chitosan membrane, two broad peaks located at about $2\theta = 10.1°$ (form I) and 20.25° (form II) are observed (Samuels, 1981) as shown in Fig. 5(a). As the calcium phosphate particles were added into the chitosan, these two characteristic peaks became flatter, suggesting that the addition of calcium phosphate ceramics could increase the amorphous nature of the chitosan matrix. This is because during

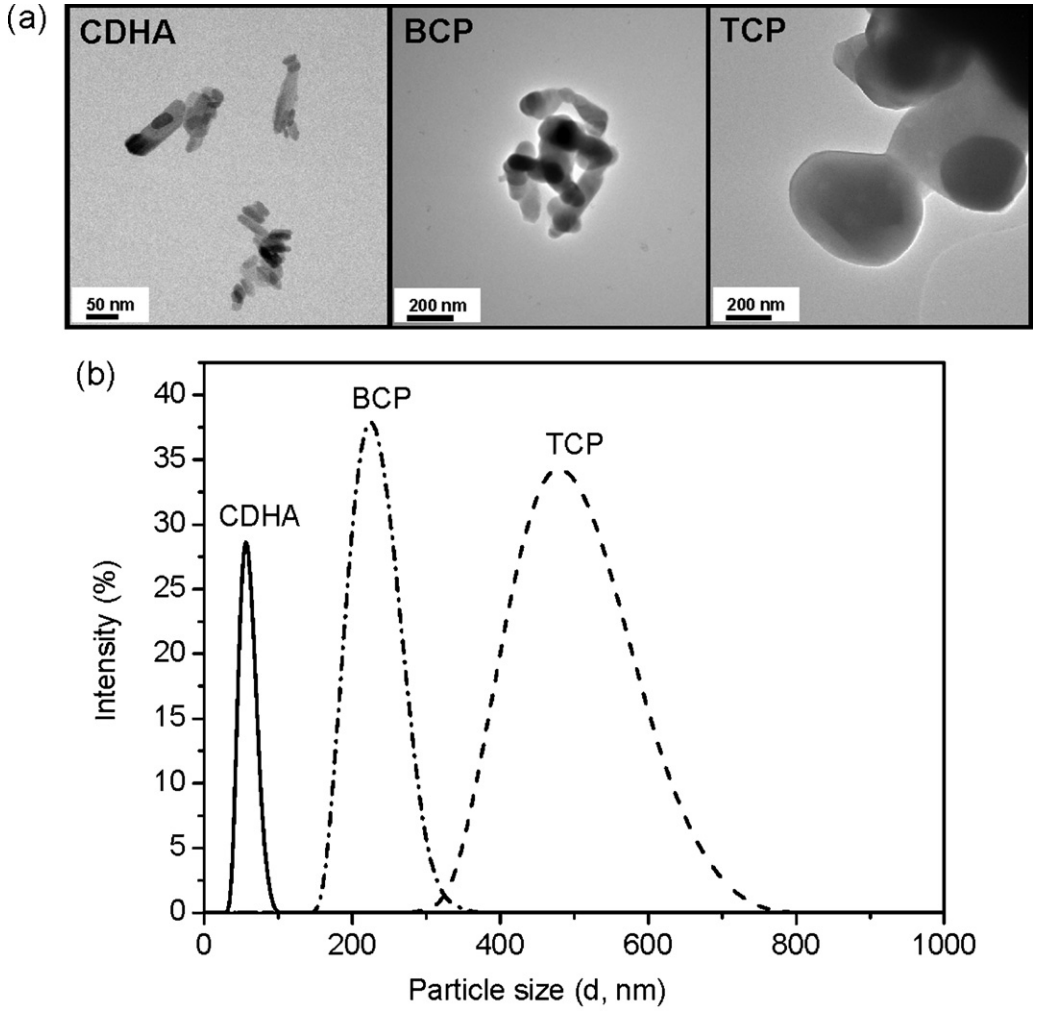

Fig. 3. TEM pictures (a) and particle size distributions (b) of the synthesized CDHA, BCP, and TCP particles.

the drying process for film formation, the presence of calcium phosphate ceramics could disrupt the interaction and the alignment of chitosan chains, and thereby decreased the crystallinity of the chitosan. On the other hand, the diffraction patterns of CDHA, BCP, and TCP in the respective composite membranes are almost the same with the spectra in Fig. 2 for the pure calcium phosphate particles, indicating the structures of the inorganic calcium phosphates did not change during the preparation of composite membranes. Fig. 5(b) shows the XRD patterns of the composite membranes after being immersed in the SBF for 24 days. The peak at $2\theta = 31.75^\circ$ due to the apatite increases in intensity in both CDHA/chitosan and BCP/chitosan membranes and appears in the TCP/chitosan membrane. This suggests that the newly deposited inorganic particles on the surface have a structure of the apatite phase.

In addition to the observation of the morphology changes on the membranes, the changes of the calcium concentration in the SBF with the incubation time were also evaluated and the results are shown in Fig. 6. The decreasing rate of the Ca^{2+} concentration in the SBF is found to be on the order of the CDHA/chitosan ≈ BCP/chitosan > TCP/chitosan > chitosan. The Ca^{2+} concentration in the SBF decreased by 13, 49, 44, and 26% for the respective chitosan, CDHA/chitosan, BCP/chitosan, and TCP/chitosan membrane after 24 days of incubation. It is clear that all membranes could uptake calcium ion and the composite membranes containing calcium phosphate ceramics have higher uptake amount of Ca^{2+} than the pure chitosan membrane. For the three composite membranes, the CDHA/chitosan and the BCP/chitosan exhibit higher Ca^{2+} adsorption than the TCP/chitosan. It was reported that the CDHA phase could induce effective nucleation and growth of the bone-like apatite in the body fluid (LeGeros, 2008). However, it is to our surprise that the BCP/chitosan membrane in which the BCP only contains 8% CDHA could also induce a noticeable amount of apatite deposition on the membrane. Based on the decreasing Ca^{2+} concentration in the SBF and the observation of the apatite particles depositing on the composite membranes, it can be deduced that the CDHA/chitosan and the BCP/chitosan composite membranes could effectively induce the formation and the deposition of the apatite particles. Both composite membranes thus have great bioactivity *in vitro* and may have the ability to bond directly to the living bone, when these materials are implanted in the body due to the same ion concentrations in the SBF and the blood plasma.

3.3. Mechanical properties of chitosan composite membranes

For the application in the guided bone regeneration such as the barrier membranes used in the treatment of periodontitis, mechanical properties of membranes are crucial. A high strength membrane is required not only for the cell attachment, proliferation, and differentiation, but also for resisting the *in vivo* stresses and loads. The pure chitosan membrane is considered to have brittle properties, as indicated in Table 1. Its elongation at break is less than 20%. The advantage of the addition of calcium phosphate particles is quite obvious that the elongation at break is greatly increased

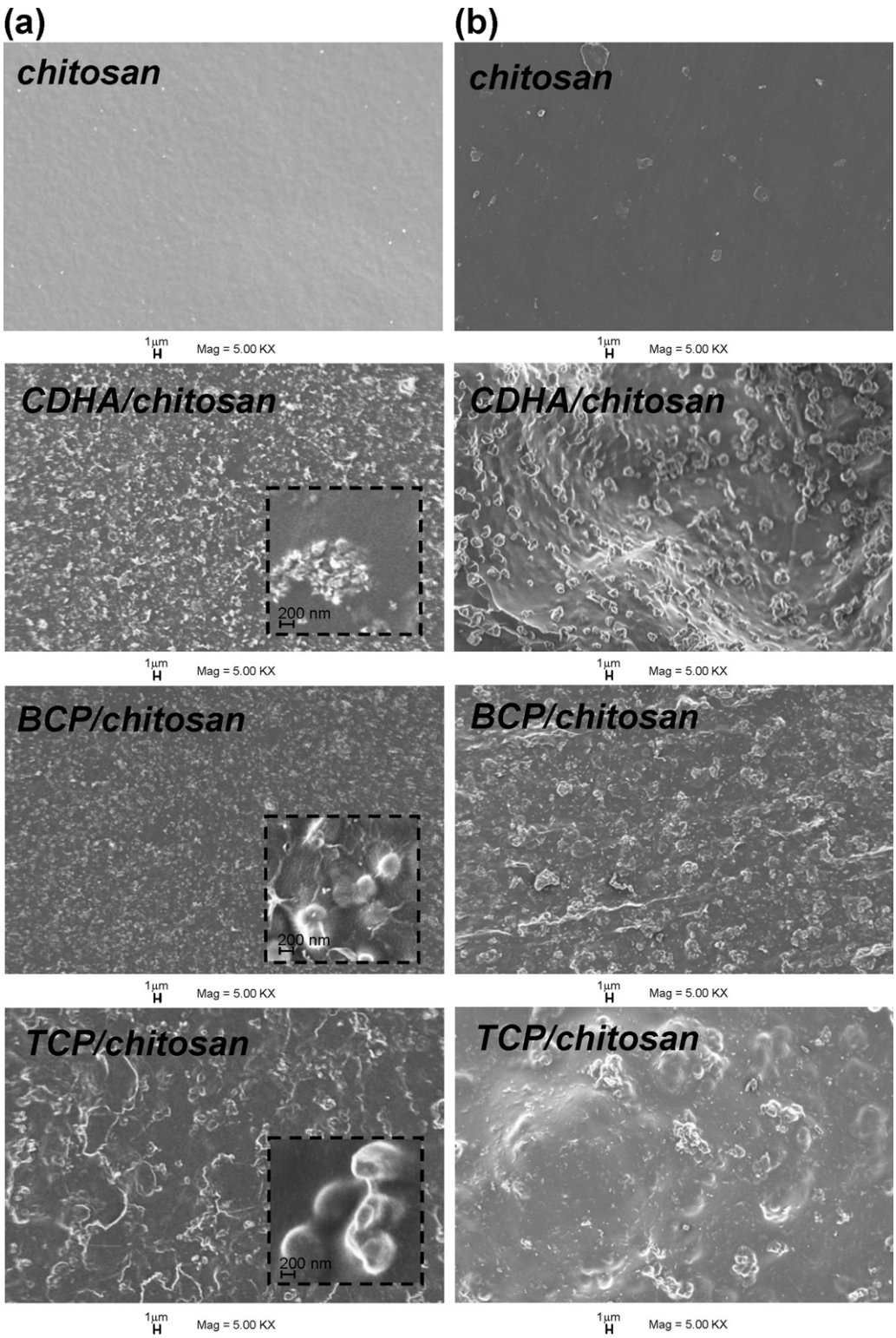

Fig. 4. SEM pictures illustrating the top surface of the chitosan, CDHA/chitosan, BCP/chitosan, and TCP/chitosan membranes before (a) and after (b) being immersed in the SBF for 24 days at 37 °C.

Table 1
Tensile mechanical properties including initial modulus (E), ultimate tensile strength (UTS), and elongation at break (ε_b) of the pure chitosan, CDHA/chitosan, BCP/chitosan, and TCP/chitosan membranes.

Tensile properties	Chitosan	CDHA/chitosan	BCP/chitosan	TCP/chitosan
E (MPa)	689 ± 43[a]	1061 ± 134	1315 ± 71	1281 ± 49
UTS (MPa)	131 ± 17	146 ± 18	239 ± 13	243 ± 21
ε_b (%)	19 ± 1	56 ± 4	113 ± 6	110 ± 8

[a] Average value and standard deviation from five determinations.

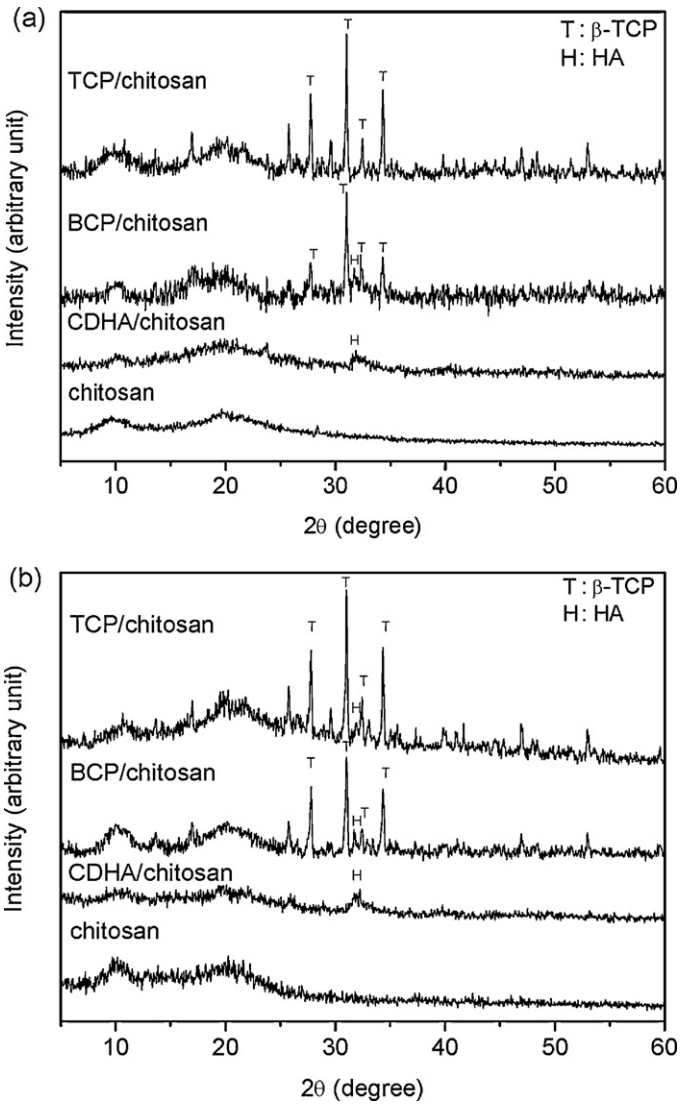

Fig. 5. XRD patterns of the chitosan, CDHA/chitosan, BCP/chitosan, and TCP/chitosan membranes before (a) and after (b) being immersed in the SBF for 24 days at 37 °C.

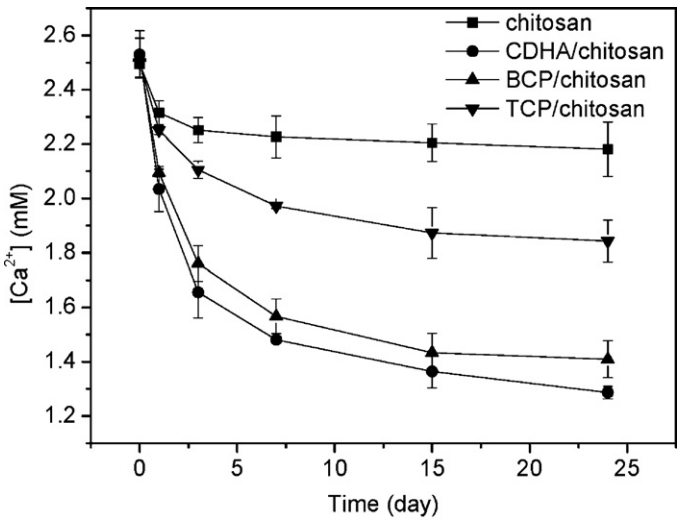

Fig. 6. The calcium ion concentration in the SBF during the immersion of various chitosan composite membranes for 24 days at 37 °C ($n = 5$).

to 56%, 113%, and 110% for the CDHA/chitosan, BCP/chitosan, and TCP/chitosan composite membranes, respectively. For their high extensible ability, both BCP/chitosan and TCP/chitosan composite membranes can be regarded as tough materials. Furthermore, the initial modulus and ultimate tensile strength are also increased by the addition of inorganic particles. The initial modulus is increased by 54% when the CDHA particles are incorporated into the chitosan, but it is increased by more than 85% with the addition of BCP or TCP particles. The ultimate tensile strength values of the BCP/chitosan and TCP/chitosan composite membranes are nearly the same and are about 1.8 times the value of the pure chitosan membrane. The result thus clearly shows that the addition of calcium phosphate particles could greatly improve the tensile mechanical properties, and it is more effective when the added calcium phosphate particles are BCP and TCP.

3.4. Osteoblast cell attachment and proliferation

For the application in the guided bone regeneration, the cell attachment and proliferation of osteoblast (OB) cells on the composite membranes were studied. The result shows that there is a significant difference in the cell culture with respect to the addition of calcium phosphate particles. The initial seeded OB cells were 5×10^4 1/mL, and the effective cell attachment was evaluated after 1, 2, 4, 5, and 6 h of culture as shown in Fig. 7(a). After 1 h of incubation, the chitosan membrane has only about 3% of the initial OB cells. However, the amounts of OB cells adhering to the composite

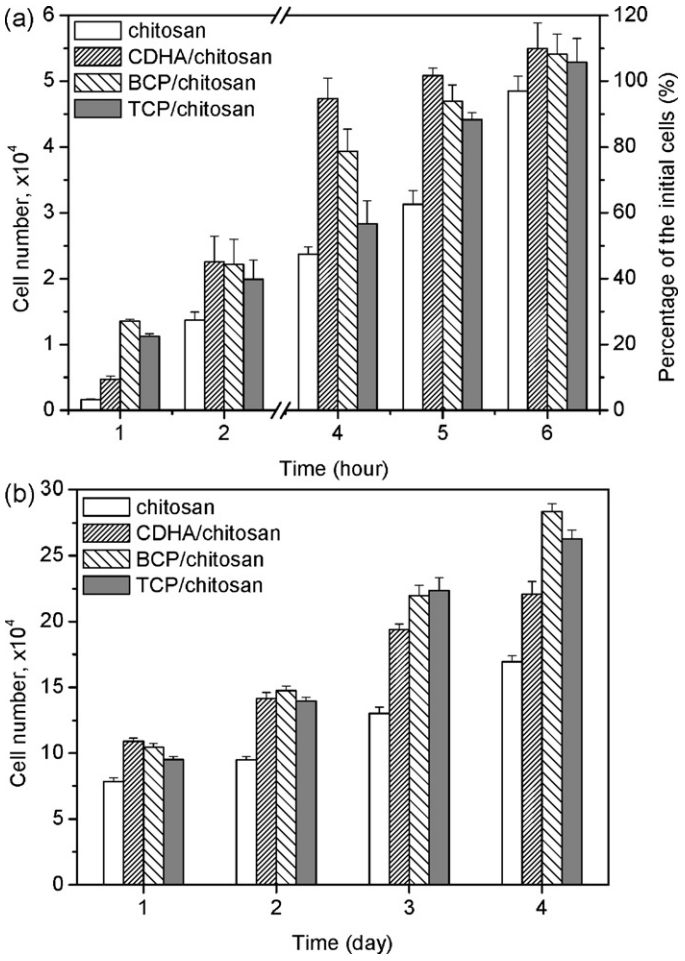

Fig. 7. The cell attachment (a) and cell proliferation (b) of OB cells cultured on the chitosan, CDHA/chitosan, BCP/chitosan, and TCP/chitosan membranes.

membranes are significantly higher than that to the chitosan membrane. After 4 h of incubation, the CDHA/chitosan membrane has the highest amount of the attached cells, approximately 95% of the initial OB cells. Still, after 6 h of culture, the amounts of the attached OB cells are almost the same on all membranes, and they are all greater than 95%. The cell attachment is known to be affected by extracellular matrix proteins. Kilpadi, Chang, and Bellis (2001) showed that the HA could adsorb some adhesive proteins such as vitronectin and fibronectin from the serum and thus increased the protein adsorption with the subsequent binding of the osteoblast precursor to the HA. The result in Fig. 7(a) proves that the addition of the CDHA could significantly increase the cell attachment on the membrane.

The cell proliferation of OB cells cultured on the composite membranes during a period of 4 days is shown in Fig. 7(b). The cell number on day 1 is higher for the composite membranes compared to the chitosan membrane, because the attachment of OB cells is superior on the composite membranes than on the pure chitosan membrane. After that, the OB cells grow rapidly and steadily with the culture time. Still, the composite membranes have higher cell viability toward OB than the pure chitosan membrane on the following days. Particularly, the BCP/chitosan and TCP/chitosan composite membranes exhibit higher proliferation of OB cells after 3 days of culture than the other two membranes. The cell number on day 4 increases by about 67% and 55% for the BCP/chitosan and TCP/chitosan membrane, respectively, when compared to the pure chitosan membrane on the same day. The steady and gradual dissolution of BCP and TCP particles might create a localized calcium- and phosphorus-rich environment, which is favorable for osteogenesis. This proves the positive effect of the TCP phase in the BCP/chitosan and TCP/chitosan membranes on bone cell proliferation. Santos, Farina, Soares, and Anselme (2009) compared the chemical influence of the HA and TCP surfaces on human osteoblast cell. They showed that the TCP could induce the higher cell proliferation, while the HA had higher cell attachment and differentiation. However, our study suggests that the BCP/chitosan composite membrane not only provides a template for osteoblast attachment, but also plays an important role for guiding osteoblast proliferation, because of the presence of both CDHA and TCP phases.

4. Conclusions

Three different calcium phosphate particles were produced based on a reverse emulsion method and the subsequent calcination. Aqueous solutions of calcium nitrate and ammonium phosphate were used as the aqueous phase, cyclohexane as the oil phase, and span 80 as the surfactant. The as-dried particles were found to be the CDHA nanoparticles with an average size of about 45 nm. These CDHA nanoparticles were further calcined at 800 °C and 1000 °C to obtain the respective BCP and TCP particles. The average particle size was increased to about 226 nm and 450 nm, respectively. Subsequently, the composite membranes combining chitosan and these calcium phosphate particles were prepared by direct-drying method. These calcium phosphate particles could modulate the mechanical properties, bioactivity, and cellular compatibility of the composite membranes. Both BCP/chitosan and TCP/chitosan composite membranes had superior tensile mechanical properties and osteoblast cell proliferation. On the other hand, the CDHA/chitosan and BCP/chitosan composite membranes could induce great bioactivity in the simulated body fluid and better osteoblast attachment. Overall, the BCP/chitosan composite membrane developed in this study has the best optimum properties and thus has the potential to be used as a barrier membrane for the periodontal treatment.

Acknowledgement

The authors would like to thank National Science Council in Taiwan for the financial support.

References

Arinzeh, T. L., Tran, T., Mcalary, J., & Daculsi, G. (2005). A comparative study of biphasic calcium phosphate ceramics for human mesenchymal stem-cell-induced bone formation. *Biomaterials*, *26*(17), 3631–3638.

Aylin, S.-U., & Russell, D. J. (2007). The addition of biphasic calcium phosphate to porous chitosan scaffolds enhances bone tissue development *in vitro*. *Journal of Biomedical Materials Research Part A*, *88A*(3), 624–633.

Behring, J., Junker, R., Walboomers, X. F., Chessnut, B., & Jansen, J. A. (2008). Toward guided tissue and bone regeneration: morphology, attachment, proliferation, and migration of cells cultured on collagen barrier membranes. A systematic review. *Odontology*, *96*(1), 1–11.

Burg, K. J. L., Porter, S., & Kellam, J. F. (2000). Biomaterial developments for bone tissue engineering. *Biomaterials*, *21*(23), 2347–2359.

Chesnutt, B. M., Viano, A. M., Yuan, Y., Yang, Y., Guda, T., Appleford, M. R., et al. (2009). Design and characterization of a novel chitosan/nanocrystalline calcium phosphate composite scaffold for bone regeneration. *Journal of Biomedical Materials Research Part A*, *88A*(2), 491–502.

Chow, L. C., & Eanes, E. D. (2001). *Octacalcium phosphate*. Basel: Karger.

Dasgupta, S., & Bose, S. (2009). Reverse micelle-mediated synthesis and characterization of tricalcium phosphate nanopowder for bone graft applications. *Journal of the American Ceramic Society*, *92*(11), 2528–2536.

Don, T.-M., Chou, S.-C., Cheng, L.-P., & Tai, H.-Y. (2011). Cellular compatibility of copolymer hydrogels based on site-selectively-modified chitosan with poly(N-isopropyl acrylamide). *Journal of Applied Polymer Science*, *120*(1), 1–12.

Etienne, O., Schneider, A., Taddei, C., Richert, L., Schaaf, P., Voegel, J.-C., et al. (2005). Degradability of polysaccharides multilayer films in the oral environment: an in vitro and in vivo study. *Biomacromolecules*, *6*(2), 726–733.

Fakhry, A., Schneider, G. B., Zaharias, R., & Senel, S. (2004). Chitosan supports the initial attachment and spreading of osteoblasts preferentially over fibroblasts. *Biomaterials*, *25*(11), 2075–2079.

Grynpas, M. D., & Omelon, S. (2007). Transient precursor strategy or very small biological apatite crystals? *Bone*, *41*(2), 162–164.

Hamilton, V., Yuan, Y., Rigney, D. A., Chesnutt, B. M., Puckett, A. D., Ong, J. L., et al. (2007). Bone cell attachment and growth on well-characterized chitosan films. *Polymer International*, *56*(5), 641–647.

Hench, L. L. (1998). Bioceramics. *Journal of the American Ceramic Society*, *81*(7), 1705–1728.

Imbronito, A. V., Todescan, J. H., Carvalho, C. V., & Arana-Chavez, V. E. (2002). Healing of alveolar bone in resorbable and non-resorbable membrane-protected defects. A histologic pilot study in dogs. *Biomaterials*, *23*(20), 4079–4086.

Jarudilokkul, S., Tanthapanichakoon, W., & Boonamnuayvittaya, V. (2007). Synthesis of hydroxyapatite nanoparticles using an emulsion liquid membrane system. *Colloids and Surfaces A: Physicochemical and Engineering Aspects*, *296*(1–3), 149–153.

Kilpadi, K. L., Chang, P.-L., & Bellis, S. L. (2001). Hydroxyapatite binds more serum proteins, purified integrins, and osteoblast precursor cells than titanium or steel. *Journal of Biomedical Materials Research*, *57*(2), 258–267.

Kuo, S. M., Chang, S. J., Niu, G. C.-C., Lan, C.-W., Cheng, W. T., & Yang, C. Z. (2009). Guided tissue regeneration with use of β-TCP/chitosan composite membrane. *Journal of Applied Polymer Science*, *112*(5), 3127–3134.

Kwon, S.-H., Jun, Y.-K., Hong, S.-H., & Kim, H.-E. (2003). Synthesis and dissolution behavior of β-TCP and HA/β-TCP composite powders. *Journal of the European Ceramic Society*, *23*(7), 1039–1045.

LeGeros, R. Z. (2008). Calcium phosphate-based osteoinductive materials. *Chemical Reviews*, *108*(11), 4742–4753.

Lin, F.-H., Liao, C.-J., Chen, K.-S., Sun, J.-S., & Lin, C.-P. (2001). Petal-like apatite formed on the surface of tricalcium phosphate ceramic after soaking in distilled water. *Biomaterials*, *22*(22), 2981–2992.

Müler, L., & Müler, F. A. (2006). Preparation of SBF with different content and its influence on the composition of biomimetic apatites. *Acta Biomaterialia*, *2*(2), 181–189.

Pattanayak, D. K., Dash, R., Prasad, R. C., Rao, B. T., & Mohan, T. R. R. (2007). Synthesis and sintered properties evaluation of calcium phosphate ceramics. *Materials Science and Engineering: C*, *27*(4), 684–690.

Petrov, O. E., Dyulgerova, E., Petrov, L., & Popova, R. (2001). Characterization of calcium phosphate phases obtained during the preparation of sintered biphase Ca-P ceramics. *Materials Letters*, *48*(3–4), 162–167.

Rinaudo, M. (2006). Chitin and chitosan: properties and applications. *Progress in Polymer Science*, *31*(7), 603–632.

Samuels, R. J. (1981). Solid state characterization of the structure of chitosan films. *Journal of Polymer Science: Polymer Physics Edition*, *19*(7), 1081–1105.

Santos, E. A. D., Farina, M., Soares, G. A., & Anselme, K. (2009). Chemical and topographical influence of hydroxyapatite and β-tricalcium phosphate surfaces on human osteoblastic cell behavior. *Journal of Biomedical Materials Research Part A*, *2*, 510–520.

Vallet-Regí, M. (2001). Ceramics for medical applications. *Journal of the Chemical Society, Dalton Transactions*, *2*, 97–108.